

phys. stat. sol. (b) **79**, 85 (1977)

Subject classification: 13.1; 13.2; 21.4

*Institut für Theoretische Physik der Technischen Universität Clausthal, Clausthal-Zellerfeld*

## Volume Dependence of the Electronic Structure of Lanthanum and Cerium

By

D. GLÖTZEL<sup>1)</sup> and L. FRITSCHÉ

Results of a band structure calculation for the f.c.c. lattices of lanthanum,  $\gamma$ - and  $\alpha$ -cerium are presented. The computation is based on Altmann's rigorous cellular method. A local potential is used generated according to the standard method. Charge densities of the free atoms are obtained from a SCFX <sub>$\alpha$</sub> -integration of the Dirac equation. Earlier band calculations using the full Slater exchange led to f-levels far too low in energy. Instead the more adequate Gaspar-Kohn-Sham value of 2/3 is used for the exchange scaling factor, which yields reasonable f-band energies. The Fermi level proves to be well below the f-bands for both metals. As follows from an analysis of the occupied band states in terms of angular momenta, there are f-admixtures of 0.3 and 0.6 electrons/atom for La and Ce, respectively, which increase slightly under pressure. As the pressure rises the Fermi level moves across three van Hove singularities in the electronic density of states at  $-15$ ,  $10$ , and at  $60$  kbar. This is also reflected in topological changes of the Fermi surface which can give rise to isostructural phase transitions. Recent Bremsstrahlung- and XPS-spectra of La and Ce are in fair agreement with the results on the density of states.

Es wird über die Ergebnisse einer Bandstrukturrechnung für die k.f.z. Gitter von Lanthan;  $\gamma$ - und  $\alpha$ -Cer berichtet. Den Rechnungen liegt die strenge Zellarmethode von Altmann zugrunde. Das Gitterpotential wird nach dem allgemein akzeptierten Standardverfahren konstruiert. (Austauschpotential in lokaler Näherung). Die dazu erforderlichen Gesamtladungsdichten der freien Atome werden durch SCFX <sub>$\alpha$</sub> -Integration der Dirac-Gleichung bestimmt. Frühere Bandrechnungen anderer Autoren, bei denen für den Austauschparameter  $\alpha$  der von Slater vorgeschlagene Wert ( $\alpha = 1$ ) benutzt wurde, ergeben viel zu niedrig liegende f-Bänder. Der benutzte Wert  $\alpha = 2/3$  nach Gaspar bzw. Kohn und Sham führt dagegen auf vernünftige f-Bandenenergien. Die Lage der Fermi-Energie ergibt sich für beide Metalle klar unterhalb dieser f-Bänder. Eine Drehimpulszerlegung der besetzten Bandzustände liefert f-Beimischungen von 0,3 bzw. 0,6 Elektronen pro Atom für La bzw. Ce, die unter hydrostatischem Druck schwach zunehmen. Mit anwachsendem Druck wandert das Fermi-Niveau nacheinander über drei van Hove-Singularitäten der elektronischen Zustandsdichte und zwar bei  $-15$ ,  $10$  und bei  $60$  kbar. Dies macht sich auch in topologischen Änderungen der Fermi-Fläche bemerkbar, die zu isostrukturellen Phasenübergängen Anlaß geben können. Neuere Bremsstrahlungs- und XPS-Messungen sind in guter Übereinstimmung mit den berechneten Zustandsdichten.

### 1. Introduction

There are a number of interesting features which make lanthanum and cerium particularly attractive as a border line case of rare-earth metals. Lanthanum, for example, is conventionally listed in the third column of the Periodic Table below yttrium, but has a melting temperature  $600$  K lower than the preceding metals in this column. Also its Debye temperature is distinctly lower. In addi-

<sup>1)</sup> Present address: Institut für Festkörperforschung der Kernforschungsanlage D-5170 Jülich, BRD.

tion, La is superconducting below 6 K, a property otherwise not met with the metals of the third column under normal conditions. At low temperatures La is stable only in the double h.c.p. lattice structure common to other light rare-earth metals. Other unusual properties like its high specific heat, its negative thermal expansion coefficient, its phase diagram etc. add evidence that it might be misplaced in this column. Cerium above a pressure of 7 kbar displays similar features, and it has been inferred from these properties that both metals have to be regarded as essentially 4f rare-earth metals. If this is to be taken for granted, a band calculation for those crucial f-electrons would seem questionable since correlation effects for f-electrons are expected to be so large that a one-particle description is believed to be inappropriate. On the other hand, for metals of this border line situation in the Periodic Table a band calculation may well come to the result, that the occupied bands contain the formerly atomic f-states only as hybridization admixtures to otherwise d-like bands. In this case a band calculation is still meaningful. As will be shown in Section 4 for the f.c.c. structures of the two metals, the occupied bands are in fact of this type.

Apart from this question as to whether or not there are occupied f-bands (characterized by a dominant f-part of the respective band states) a detailed band structure and the associated density of states can also give hints for isostructural lattice instabilities under hydrostatic pressure. Recent experiments on La by Balster and Wittig [1] suggest that the observed peak of the residual resistivity at 53 kbar might be attributed to an isostructural phase transition. As has been pointed out by Lifshits [2], such phase transitions may occur if the Fermi energy is shifted across a van Hove singularity of the electronic density of states.

## 2. Method of Calculation

The advantages of the rigorous cellular method due to its simple mathematical form and its remarkable accuracy has been emphasized by Altmann various times (see e.g. Altmann [3], cf. also Fritsche and Rafat-Mehr [4]). If one wants to classify band states according to their hybridization, that is according to the mixing of the original atomic states, Altmann's method proves to be ideally suited, since the wave function  $\psi(\mathbf{r})$  is represented by only one expansion in terms of atom-like functions

$$\psi(\mathbf{r}) = \sum_{l=0}^L \sum_{m=-l}^l c_{lm} R_l(E, r) Y_{lm}(\hat{\mathbf{r}}).$$

Here the usual notation for the spherical harmonics  $Y_{lm}$  and for the radial part  $R_l(E, r)$  of the wave function has been used. Each  $R_l(E, r)$  is generated by a numerical integration of the radial part of the Schrödinger equation at energy  $E$ , and hence  $\psi(\mathbf{r})$  itself solves the Schrödinger equation for the same energy everywhere in the cell. The expansion coefficients  $c_{lm}$  represent the sought-for mixing amplitudes. They follow directly from the secular equations obtained by minimizing the mean square mismatch of  $\psi(\mathbf{r})$  at the cell boundaries. The convergence of the expansion is relatively fast. If it is broken off at a maximum angular momentum of  $L = 6$ , the r.m.s. deviation from the exact band structure is about 3 mRyd for a d-band metal. Due to the simple structure of the wave function in the entire cell relativistic corrections such as the mass velocity and the Darwin term can be easily obtained by forming the respective

expectation values. These corrections shift the s-p states to lower energies much stronger than the d- and f-states, thereby enlarging the s-p admixture to the occupied states. On the other hand, the effect of spin-orbit coupling is an order of magnitude smaller and hence was neglected within the band calculation.

To calculate the density of states the "cellular band structure" along the main symmetry directions was extrapolated into the fundamental wedge of the Brillouin zone by means of a combined OPW tight-binding scheme (see e.g. [5 to 7]) which had to be extended to include f-bands.

On fitting the 47 parameters of the associated model Hamiltonian, points in the vicinity of the Fermi energy were preferable weighted to keep the approximation error below 10 mRyd in this region. The computation of the density of states was finally carried out by partitioning the fundamental wedge in 5333 cubes and using the method of Gilat and Raubenheimer [8].

### 3. Generation of the Lattice Potential

The lattice potential was constructed along the lines of Mattheiss' method [9]. To this purpose the charge densities of the respective free atoms had to be superimposed. They were obtained from a Dirac-SCFX<sub>α</sub> calculation based on the program of Liberman et al. [10]. The muffin-tin form of the total potential in each cell was arrived at by using the standard methods. Both for the free atom and for the lattice the scaling factor  $\alpha$  in the local exchange potential was chosen to be 2/3 in accordance with the Gaspar-Kohn-Sham value. The electron configurations used for the free atoms of La and Ce, respectively, were the following:

$$\begin{array}{cc} \text{La} & \text{Ce} \\ 4f^0 5d^1 6s^2, & 4f^1 5d^1 6s^2. \end{array}$$

The mutual mixing of these states in forming the occupied band states results in a reconfiguration of the form

$$\begin{array}{cc} \text{La} & \text{Ce} \\ 4f^\epsilon(5d, 6s, 6p)^{3-\epsilon}, & 4f^\epsilon(5d, 6s, 6p)^{4-\epsilon}, \end{array}$$

where

$$\epsilon = \begin{cases} 0.3 & \text{for La,} \\ 0.6 & \text{for Ce} \end{cases}$$

at normal pressure.

As can be seen from the change of configuration after the first step, a self-consistent band calculation would yield a smaller value of  $\epsilon$  for La and a larger one for Ce.

### 4. Results

The band structure of f.c.c. La at 0 kbar for special directions of the Brillouin zone is shown in Fig. 1. Obviously the lowest band starts free-electron-like at  $\Gamma_1$  and reaches a maximum as d-like contributions become dominant. The Fermi energy (dashed line) cuts the second band and is just below a saddle point in this band on the symmetry line  $\Sigma$ . The general features of the band structure are schematically shown in Fig. 2, where hybridization effects have been omitted for clarity. The d-band region spreads over a range of about 10 eV, whereas the f-bands lie within a relatively narrow range of 1.2 eV width. The Fermi energy is clearly below this f-band region. On applying a rather high

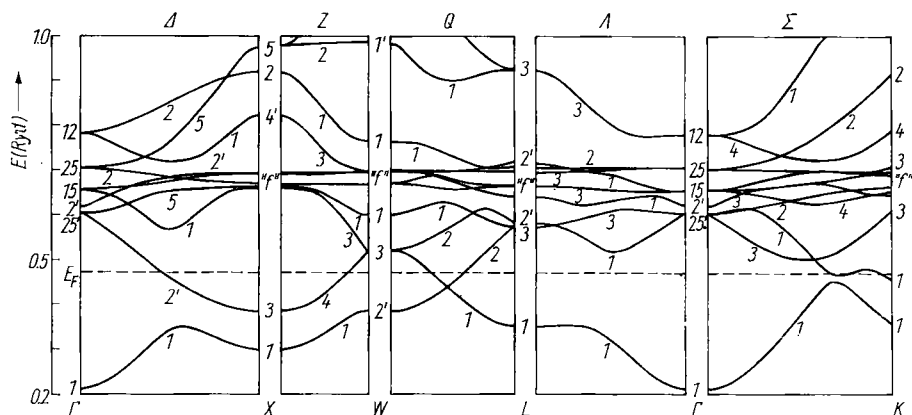


Fig. 1. Band structure of f.c.c. La obtained from the cellular method

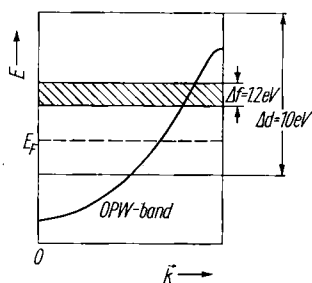


Fig. 2. Band structure of a d-f band metal schematically

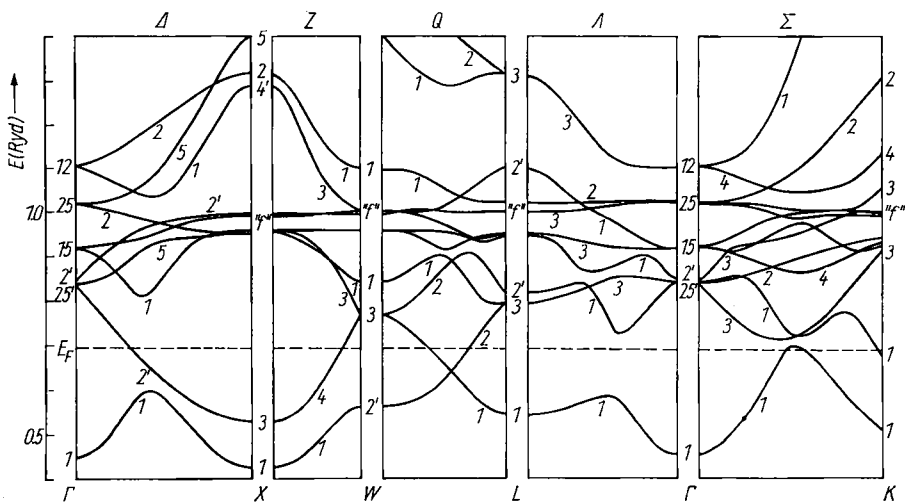


Fig. 3. Band structure of f.c.c. La at 120 kbar obtained from the cellular method. (Note that at this pressure the point of intersection of the Fermi level with the second band is shifted towards the origin along the  $\Delta$ -direction)

pressure of 120 kbar<sup>2)</sup> the band structure is noticeably changed, but not basically, as can be seen from Fig. 3. The Fermi energy is now below the maximum of the first band on the symmetry line  $\Sigma$  and the f-band range has been considerably widened.

An angular momentum analysis of the first two bands along the  $\Delta$ -direction is shown in Fig. 4a, b. The effect of hybridization for the first band is clearly

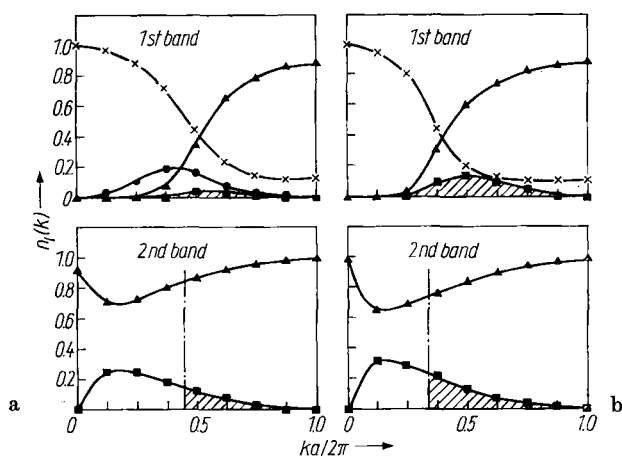


Fig. 4. Angular momentum analysis of the first two bands along the  $\Delta$ -direction a) at normal pressure, b) at 120 kbar.  $\times$  s-contribution,  $\bullet$  p-contribution,  $\blacktriangle$  d-contribution,  $\blacksquare$  f-contribution. (As regards the shift of the Fermi wave vector at higher pressure see comment to Fig. 3.)

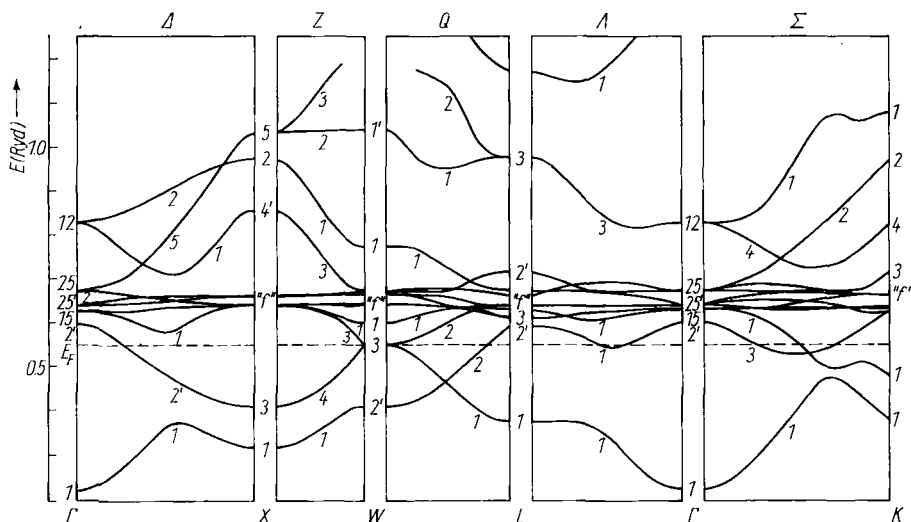


Fig. 5. Band structure of  $\gamma$ -Ce obtained from the cellular method

<sup>2)</sup> The lattice constant of La at 120 kbar has been obtained from recent experiments by Syassen and Holzapfel [11]. The respective values for  $\alpha$ - and  $\gamma$ -cerium and for f.c.c. lanthanum were taken from Pearson's handbook [12]. For each pressure the lattice potential was anew generated according to the associated lattice constant.

demonstrated. Obviously the character of the band states changes from almost pure s-like at the  $\Gamma$ -point to almost pure d-like at the zone boundary. By contrast, the second band is dominantly d-like with a small f-admixture. The shaded areas refer to f-contributions to occupied band states. As can be seen from Fig. 4b, these f-contributions increase with increasing pressure. Not surprisingly, the band structure of  $\gamma$ -Ce shown in Fig. 5 displays essentially the same features as the one of La. However, the f-bands narrow by about 20% and the distance of their centre of gravity from the Fermi level is reduced by a factor of two. Furthermore, the lowest unoccupied level at the  $\Gamma$ -point changes from 5d to 4f character corresponding to the representations  $\Gamma_{25'}$  and  $\Gamma_{2'}$ , respectively.

### 5. Comparison with Experiments

Since de Haas-van Alphen measurements on the Fermi surfaces of La and Ce appear to be not yet feasible, experiments directly involving the density of states provide the only source of data which our results can be compared with. Fig. 6a, b shows the density of states for La at normal pressure and 120 kbar. The contributions according to the angular momenta of atom-like states which hybridize into the band states, are plotted separately. Experimental data on the density of states at the Fermi surface obtained from specific heat measurements may be compared with our results. For f.c.c. La and  $\gamma$ -Ce at normal pressure and for  $\alpha$ -Ce we find (in units of states/(atom Ryd)):

$$26.8, \quad 19.1, \quad 11.6,$$

whereas the experimental values are (cf. [13 to 15]):

$$66.4^3), \quad 41.9, \quad 73.9.$$

Thus the electron phonon enhancement  $\lambda$  defined by  $\gamma_{\text{exp}} = \gamma_0(1 + \lambda)$  for f.c.c. La equals 1.5 and is very strong as one might expect from the superconducting

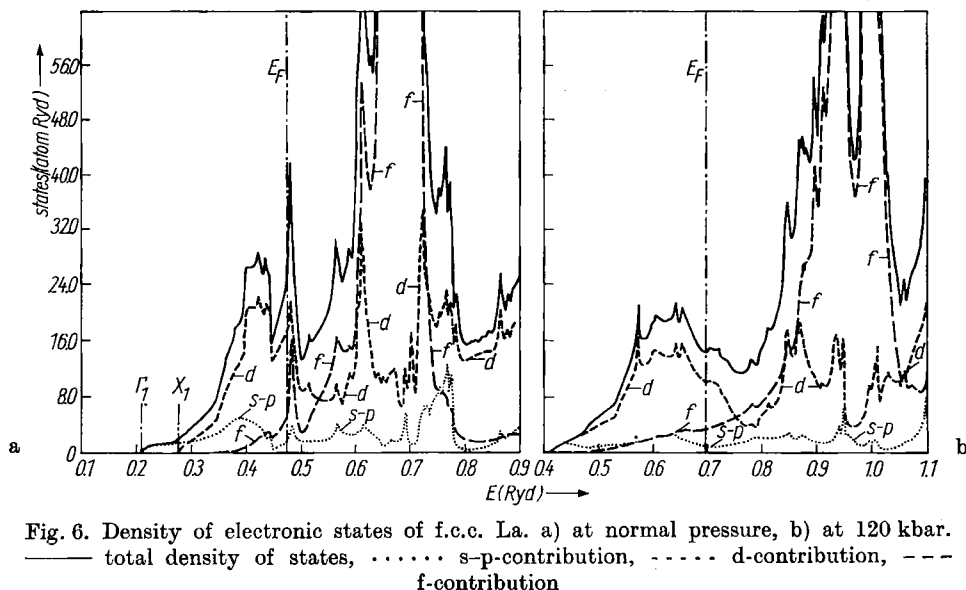


Fig. 6. Density of electronic states of f.c.c. La. a) at normal pressure, b) at 120 kbar. — total density of states, ..... s-p-contribution, - - - - d-contribution, - - - f-contribution

<sup>3)</sup> Unfortunately this value has been quoted a factor two too small in earlier theoretical work [16], which yielded a misleading agreement between theory and experiment.

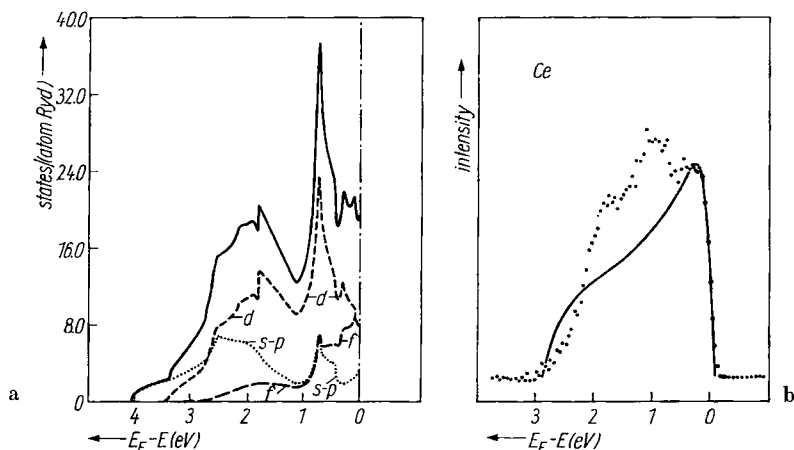


Fig. 7. a) Occupied density of states for  $\gamma$ -Ce (this work). The total density of states and the various  $l$ -dependent contributions are marked as in Fig. 6a, b. b) XPS spectrum of Ce [20] (dotted curve). This spectrum is to be compared with the solid curve in Fig. 7a)

properties. The disagreement in the case of  $\gamma$ - and especially  $\alpha$ -Ce might be due to wrong placement of the 4f band as well as to strong enhancement.

Recent X-ray emission spectra of La and Ce [17, 18] display a well defined peak at 5.5 and 3.1 eV, respectively, below the continuum limit, which very likely reflects a corresponding peak in the unoccupied density of states. In fact, our calculation yields a very high 4f density of states centered around 2.7 and 1.2 eV, respectively, from the Fermi level. While the numerical agreement is not satisfactory, the experimental results confirm our findings, that the pure f-bands lie well above the Fermi energy.

XPS measurements by Baer and Busch [19] on La and Ce support fairly well some details of our density of states. For the XPS spectrum of La [19] the authors find a peak at about 0.6 eV below the Fermi energy which compares well with the peak at 1 eV in our density of states. For Ce the agreement is even more striking, as can be seen from Fig. 7a, b where the occupied region of the density of states is shown in comparison with the XPS spectrum of [20]. Hence, there seems to be no need for a localized f-level below the Fermi energy to explain the spectrum.

### Acknowledgement

We express our gratitude to the Deutsche Forschungsgemeinschaft for generous financial support which made the present study possible.

### References

- [1] H. BALSTER and J. WITTIG, *J. low-Temp. Phys.* **21**, 377 (1975).
- [2] J. M. LIFSHITS, *Soviet Phys. — J. exper. theor. Phys.* **11**, 1130 (1960).
- [3] S. L. ALTMANN, in: *Orbital Theories of Molecules and Solids*, Ed. N. H. MARCH, Clarendon Press, Oxford 1974 (p. 30).
- [4] L. FRITSCHÉ and M. RAFAT-MEHR, *Internat. J. Quantum Chem.* **S8**, 457 (1974).
- [5] L. HODGES, H. EHRENREICH, and N. D. LANG, *Phys. Rev.* **152**, 505 (1966).
- [6] F. M. MUELLER, *Phys. Rev.* **153**, 659 (1967).
- [7] N. H. SMITH and L. F. MATTHEISS, *Phys. Rev. B* **9**, 1341 (1974).

- [8] G. GILAT and L. J. RAUBENHEIMER, Phys. Rev. **144**, 390 (1966).
- [9] L. F. MATTHEISS, Phys. Rev. **133**, A 1399 (1964).
- [10] D. A. LIBERMAN, D. T. CROMER, and J. T. WABER, Computer Phys. Commun. **2**, 107 (1971).
- [11] K. SYASSEN and W. B. HOLZAPFEL, Solid State Commun. **16**, 533 (1975).
- [12] W. B. PEARSON, A Handbook of Lattice Spacings and Structures of Metals and Alloys, Pergamon Press, London/New York 1958.
- [13] D. C. JOHNSON and D. K. FINNEMORE, Phys. Rev. **158**, 376 (1967).
- [14] K. A. GSCHNEIDNER JR., in: Encyclopedia of the Chemical Elements, Ed. C.A. HAMPEL, Van Nostrand Co., New York 1968 (p. 119).
- [15] D. C. KOSKIMAKI and K. A. GSCHNEIDNER JR., Phys. Rev. B **11**, 4463 (1975).
- [16] H. M. MYRON and S. H. LIU, Phys. Rev. B **1**, 2414 (1970).
- [17] R. J. LIEFELD, A. F. BURR, and M. B. CHAMBERLAIN, Phys. Rev. A **9**, 316 (1974).
- [18] M. B. CHAMBERLAIN, A. F. BURR, and R. J. LIEFELD, Phys. Rev. A **9**, 663 (1974).
- [19] Y. BAER and G. BUSCH, Phys. Rev. Letters **31**, 35 (1973).
- [20] Y. BAER and G. BUSCH, J. Electr. Spectroscopy rel. Topics **5**, 611 (1974).

*(Received September 16, 1976)*